The parametrical nonlinear analysis of embedded retaining structure

Helena Vrecl Kojc and **Stanislav Škrabl**
Faculty of Civil Engineering, University of Maribor, Smetanova ulica 17, SI-2000 Maribor, SLOVENIA
e-mail: helena.vrecl.kojc@uni-mb.si; stanislav.skrabl@uni-mb.si

SUMMARY

The paper presents the generalized model of soil-structure interaction of an embedded retaining structure. The presented solution is based on an elasto-plastic analysis of the interaction between a retaining structure and non-linear soil. The plane strain model of the structure and soil is analysed using the finite element method. Based on the results of analytical solutions and numerical analyses, a generalized model of interaction analysis between the structure and soil has been developed. The significance of the proposed model is reflected above all in the fact that deformations and inner forces of the structure with different soil characteristics and geometrical data are based on a limited number of non-linear analyses [1]. The results of the research are presented in the form of diagrams.

The second part of the paper presents an example of a real geotechnical problem with the verification of the generalized results and design diagrams for the use in the design practice.

Key words: *soil-structure interaction, retaining structure, elasto-plastic analysis, non-linear analysis.*

1. INTRODUCTION

Interdependence between loads and deformations of the retaining structure depends above all: (a) on the properties of the embedded retaining structure with the consideration of the slope load action due to the excavation in front of the structure, (b) conditions of the soil resistance after the excavation which depend on the structure deformations, and (c) undloading elasto-plastic constitutive properties of the soil.

The use of non-linear constitutive inter-dependencies of soils ensures more realistic results [2]. In such cases, the problems of shear resistance control at the structure and the generation of a finite element mesh around it appear and they can both fundamentally influence the results of the numerical analysis. Therefore, we have used contact elements of a virtual thickness along the contact surface between the structure and the soil, which makes it possible to verify the shear strength activation and to refine the finite element mesh. A generalized numerical soil-structure model has been developed which is based on a supplementary interaction analysis procedure performed in this manner.

Generalized solutions presented in the paper can be useful in the design of simple geotechnical problems in practice.

2. GENERALIZED SOIL-STRUCTURE MODEL

The interdependence between the loads and movements of the retaining structure is determined by using the results of numerical analyses and a generalized model which is presented in Figure 1.

The influence region of twice the wall height under the retaining structure as well as left and right from the retaining structure ($\bar{h} = 2\bar{H}$ and $\bar{L} = 2\bar{H}$; $\bar{H}$ denotes the generalized excavation depth) was considered in the analyses. The interaction analyses were performed with regard to the generalized parameters: unit weight of the soil $\bar{\gamma} = \gamma / \gamma = 1$ and the structure $\bar{\gamma}_c = \gamma_c / \gamma = 1.25$, generalized cohesion shear strength of the soil $\bar{c} = c/(\gamma H)$ and generalized surcharge $\bar{q} = q/(\gamma H)$.
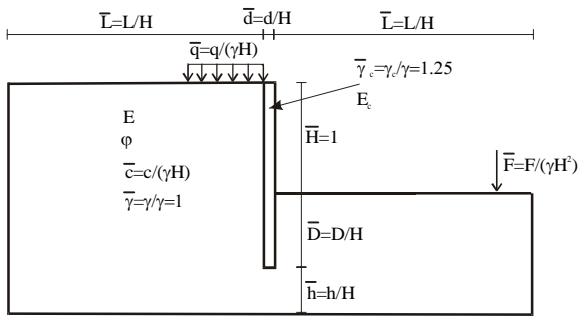
Fig. 1 Generalized model of the soil-structure interaction analysis

3. ELASTO-PLASTIC SOLUTION

The model is analyzed using the finite element method under elasto-plastic conditions [3]. We used the non-dimensional elements along the soil-structure contact surface. The relationships between joint loads and deformations were assessed using the following expression:

$$d\bar{f} = \bar{K}\,d\bar{u} \qquad (1)$$

where $d\bar{f}$ represents the vector of the load rate, and $d\bar{u}$ the vector of the deformation rate at the joint of the soil-structure contact which is made discrete in terms of finite elements, while $\bar{K}$ denotes the elasto-plastic stiffness matrix of the structure. The matrix $\bar{K}$ is evaluated for each calculation increment:

$$\bar{K} = \int_{\bar{V}} \bar{B}^T\, \bar{C}^{ep}\, \bar{B}\, d\bar{V} \qquad (2)$$

where $\bar{V}$ denotes the volume of the generalized structure, $\bar{B}$ the strain interpolation function, and the $\bar{C}^{ep}$ elasto-plastic constitutive matrix of the structure and foundation soil, including the surface contact elements between the structure and the soil [4]:

$$\bar{C}^{ep} = \bar{C}^{ep}\left(E, \nu, \sigma'_{ij}, \varphi, c, \varepsilon^{pl}\right) \qquad (3)$$

where σ'_{ij} denotes the stress state in the soil and ε^{pl} denotes the vector of plastic deformations which depends on the yield rule and soil hardening or softening. For elasto-ideal-plastic material and soils with hyperbolically deformational hardening, the values of the constitutive elasto-plastic matrix are transformed in all transformations of the real structures into generalized ones (see Figure 1).

When transforming the generalized interdependencies into a real elasto-plastic soil-structure interaction, expression (1) can be given as follows:

$$\begin{aligned} df &= \left(\gamma H/\bar{H}\right)\left(H/\bar{H}\right)d\bar{f} = \\ &= \left(H/\bar{H}\right)\bar{K}\left(\gamma H/\bar{H}\right)d\bar{u} = K\,du \end{aligned} \qquad (4)$$

Equation (4) is a basis for transforming the generalized interdependencies into real problems [5].

We can make analyses using generalized models by considering generalized loading, generalized unit weight, cohesion and generalized geometrical data.

4. THE ISOTROPIC HARDENING SOIL MODEL

The analyses were performed by using the Hardening-Soil (non-linear) model. In contrast to an elastic perfectly-plastic model, the yield surface of a hardening plasticity model is not fixed in the principal stress space, but it can expand due to plastic strain. A distinction can be made between the two main types of hardening, namely shear hardening and compression hardening. Shear hardening is used to model irreversible strains due to primary deviatory loading. Compression hardening is used to model irreversible plastic strains due to primary compression in both oedometer loading and isotropic loading. Both types of hardening are contained in the present model [6].

The Hardening-Soil model is an advanced model for simulating the behaviour of different types of soil, both soft soils and stiff soils [7]. When subjected to primary deviatory loading, the soil shows a decreasing stiffness and irreversible plastic strains develop simultaneously. In the special case of a drained triaxial test, the observed relationship between the axial strain and the deviatoric stress can be well approximated by a hyperbola. Such a relationship was first formulated by Kondner [8] and later used in the well-known hyperbolic model [9]. A basic feature of the present Hardening-Soil model is the stress dependency of soil stiffness. Since we used the Hardening-Soil model in our analyses the solution is called a "non-linear solution".

5. INPUT PARAMETERS

The size of the model was chosen on the base of the influenced area of the embedded retaining structure (see Figure 2). The final generalized excavation depth is one unit ($\bar{H}$) and the maximum generalized embedment of the structure is $\bar{D} = 2\bar{H}$.

The retaining structure is taken as an elastic beam element that is defined by the thickness of the structure and the material characteristics of the concrete (w, EA, EI).

In our analyses a commercial computer code Plaxis-Version 7.2 was used [6]. The program allows for a fully automatic generation of a finite element mesh, with the option of global or local refinement. The mesh consists of 6-node triangular elements (see Figures 3 and 4). The decision for such geometry and mesh generation is based

on several preliminary researches [10]. The analyses were made on different models with the following variables: (a) the characteristic soil parameters are shear characteristics with $15° < \varphi < 45°$, $\bar{c} = 0.005$ and a stiffness soil modulus of $E_{50}^{ref} = E = 30\ MPa$ (*10 MPa, 100 MPa*) and (b) parameters of the retaining structure with $\bar{D} = 0.50$ (*0.75, 1.00, 1.50, 2.00*), $\bar{d} = 0.10$ and concrete stiffness modulus $E_c = 30\ MPa$ [11].
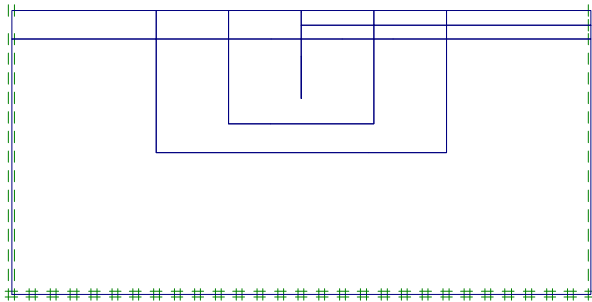
Fig. 2 Geometrical data of the model
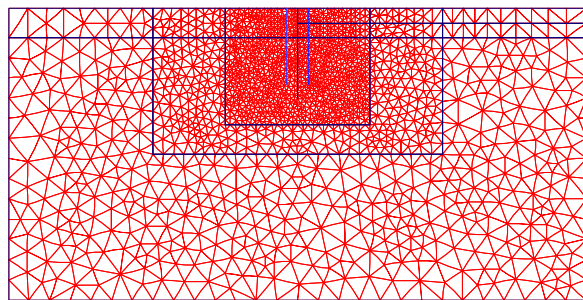
Fig. 3 Finite element mesh of the model
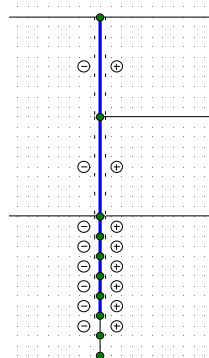
Fig. 4 Retaining structure and interface elements

6. SOLUTIONS

The solutions are indicated by the maximum displacements and inner forces (shear stresses and bending moments) of the retaining structure. They are presented by graphs in dependence between generalized soil parameters, depth of the retaining structure embedment and the friction angle of the soil. The results of analyses are: (a) generalized maximum

displacements of the retaining structure $\bar{u}_{h\,max}$, (b) generalized maximum shear force of the retaining structure $\overline{Q}_{max}$ and (c) generalized maximum bending moment of the retaining structure $\overline{M}_{max}$.

Note: the following denotations in the text and in the figures have the same meaning $\bar{u}_{h\,max} \equiv u´_{hmax}$, $\overline{Q}_{max} \equiv Q´_{max}$, $\overline{M}_{max} \equiv M´_{max}$, $\overline{D} \equiv D´$, $\bar{d} \equiv d´$, $\bar{c} \equiv c´$ (Figures 6, 7, 9 and 11).

Homogeneous non-cohesive soil with a stiffness modulus of soil $E = 30\ MPa$ has been referred to Model I (see Figure 5).
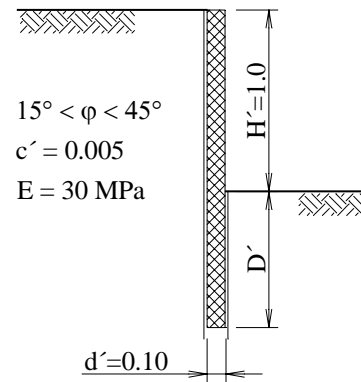
Fig. 5 Homogeneous non-cohesive soil (Model I)

The analysis results of Model I are shown in Figure 6.

The obtained results reveal the following findings: (a) the generalized displacements slightly increase for values of friction angle $35° < \varphi < 45°$ and are mostly the same for $0.75 < \overline{D} < 2.00$, for smaller embedment depths ($\overline{D} = 0.50$) the increase is essentially faster, (b) the generalized shear force slightly increases to the specific friction angle φ where it reaches the peak positive value, then it changes to a negative value which increases rapidly to the failure friction angle φ_k. The values are in the range between *0.15* and *-0.45*; for smaller embedment depths ($\overline{D} = 0.50$) their values are negative, (c) the generalized bending moments increase in the range from *0.03* to *0.20*, and (d) the failure friction angle φ_k is equal to *19°* for values of generalized embedment of structure between *1.50* and *2.00*; for $\overline{D} = 1.00$ is failure friction angle $\varphi_k = 23°$; for $\overline{D} = 0.75$ is failure friction angle $\varphi_k = 28°$; for $\overline{D} = 0.50$ is failure friction angle $\varphi_k = 34°$.

The comparison of the analyses results for Model I for different values of the embedment depth $\overline{D}$ and stiffness soil modulus E is presented in Figure 7.
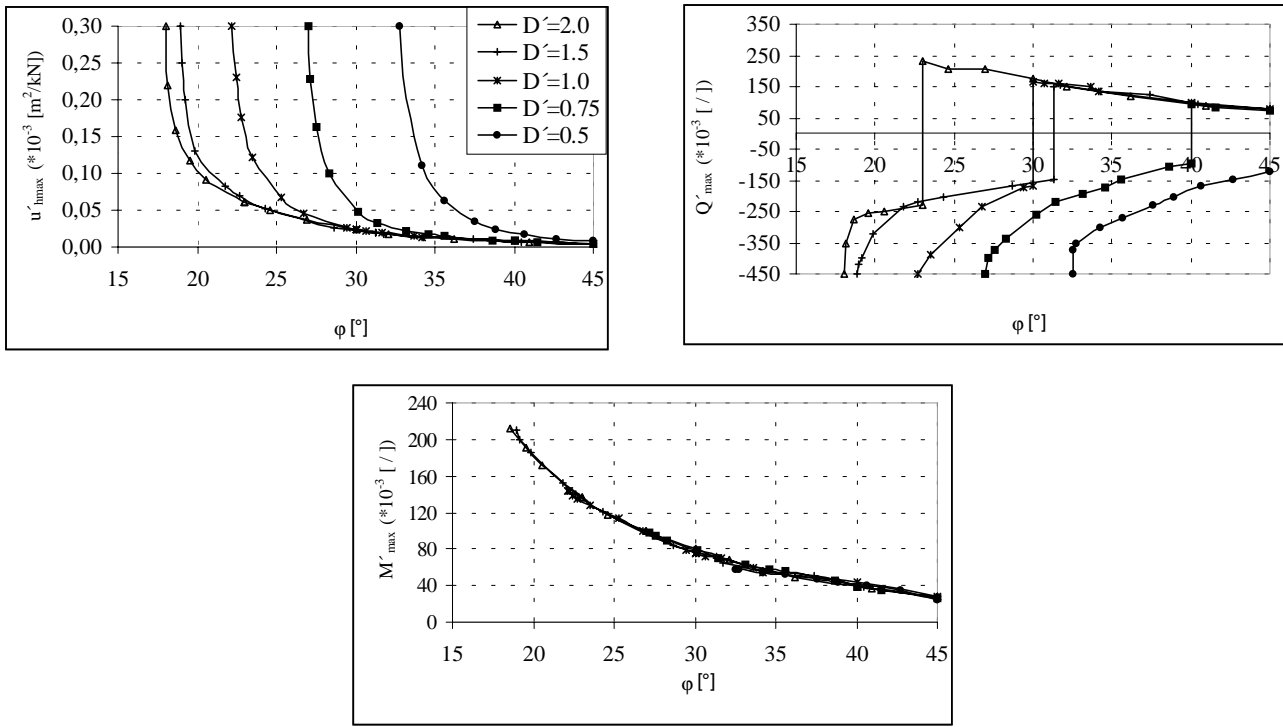
Fig. 6 Generalized displacements and inner forces of Model I
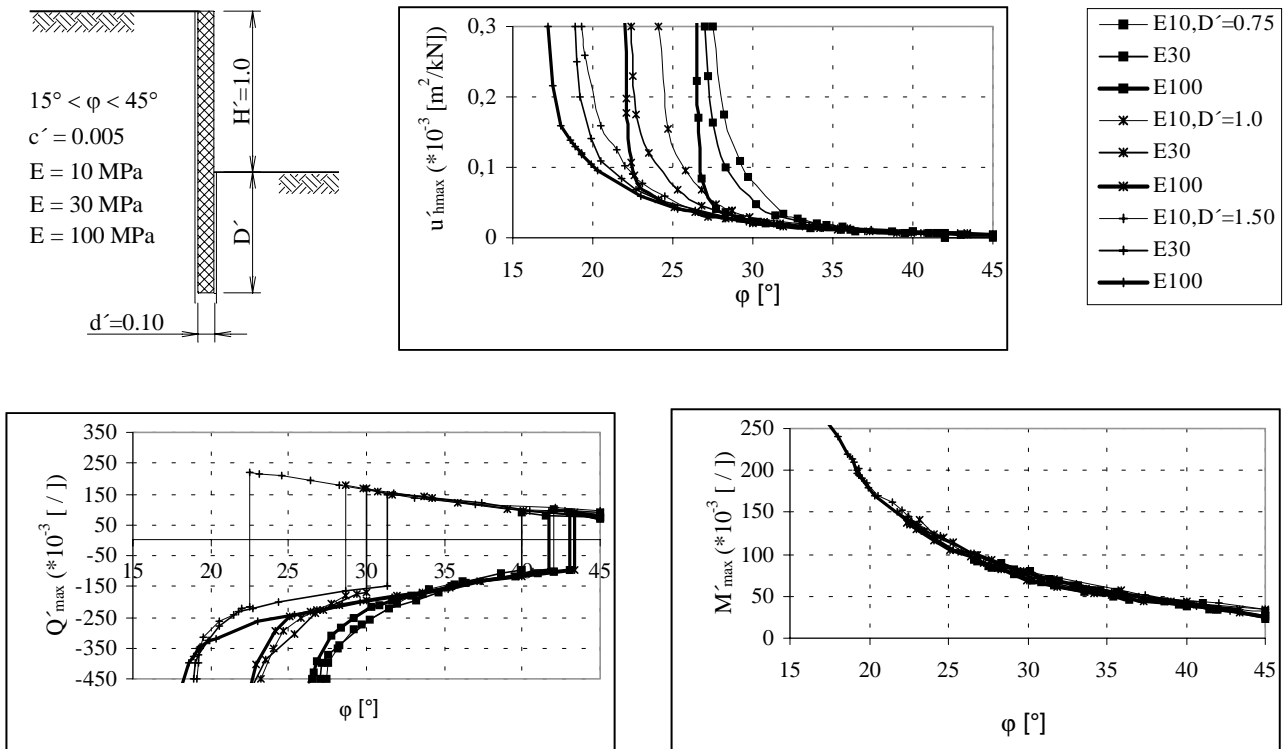
Fig. 7 Generalized displacements and inner forces of Model I for different values of $\overline{D}$ and E

On the basis of the results we can conclude: (a) the failure friction angle moves to lower values with the increasing stiffness modulus and retaining structure embedment, (b) the stiffness modulus has no influence on the generalized displacements and shear forces at $35° < \varphi < 45°$; its maximal influence is in the range of design friction angle φ_p, then the influence again decreases, and (c) the stiffness modulus has no influence on the generalized bending moments.

Homogeneous cohesive soil with a stiffness modulus $E=30$ MPa is referred to as Model II (see Figure 8).
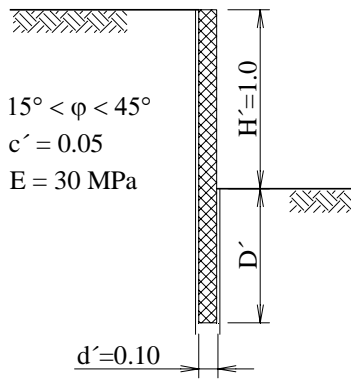
Fig. 8 Homogeneous cohesive soil (Model II)

The comparison of solutions of Model I and Model II is presented in Figure 9.
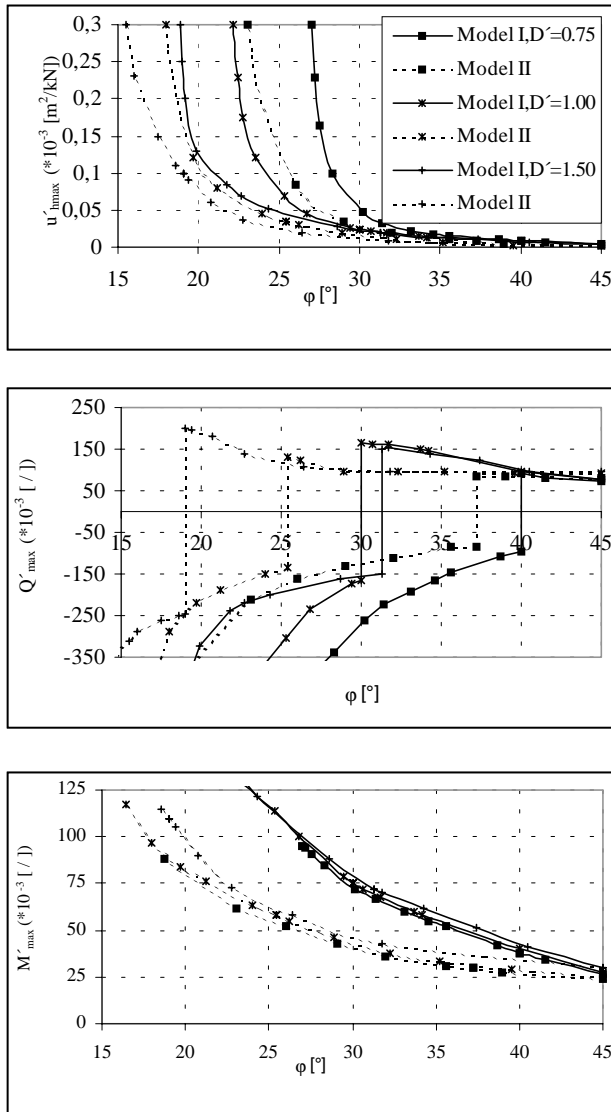
Fig. 9 The comparison of solutions of Model I and Model II

On the basis of the results we can conclude: (a) the failure friction angle moves to lower values in Model II, (b) cohesion has no influence on generalized displacements at $35° < \varphi < 45°$ after that the difference is increased and (c) cohesion has influence on the shear forces and bending moments already at $\varphi < 45°$.

The results shown in Figures 6, 7 and 9 lead to some general conclusions. The generalized displacements increase with a decreasing friction angle to the asymptote axis, which represents the critical or failure friction angle φ_k. The values of generalized shear forces change the sign for the considered generalized embedment $\overline{D}$ at a certain friction angle and then their value increases to the asymptote value. Generalized bending moments are increased by decreasing the friction angle to a maximum value at the failure friction angle. Their value does not essentially depend on the embedment depths $\overline{D}$.

7. PRACTICAL PROBLEM

The generalized non-linear solutions of soil-structure interaction can be used for designing simple geotechnical engineering problems.

The practical example is shown in Figure 10. The soil parameters of an example are: $\varphi=20.0 \ kN/m^3$, $\varphi=31°$, $E=30 \ MPa$. The retaining structure data are: $H=5.00 \ m$, $D=5.00 \ m$, $d=0.50 \ m$, $E_c=25 \ GPa$, $\gamma_c=25.0 \ kN/m^3$.
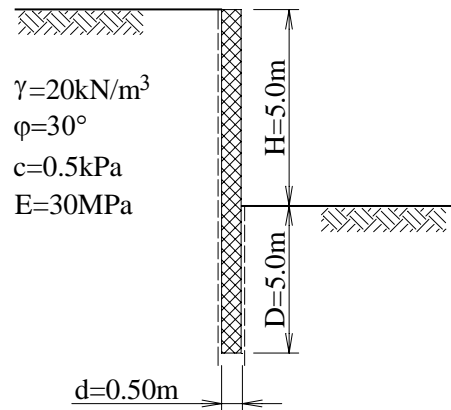
Fig. 10 Example of homogeneous soil model with an embedded retaining structure

The generalized parameters are defined from the real ones by terms:

$$\overline{D} = \frac{D}{H} \quad (5)$$

$$\overline{d} = \frac{d}{H} \quad (6)$$

$$\overline{c} = \frac{c}{\gamma \cdot H} \quad (7)$$

The real values of the maximum displacement and inner forces are calculated from the generalized ones by using the following relations:

$$\overline{u}_h = \frac{u_h}{\gamma \cdot H^2} \qquad (8)$$

$$\overline{Q} = \frac{Q}{\gamma \cdot H^2} \qquad (9)$$

$$\overline{M} = \frac{M}{\gamma \cdot H^3} \qquad (10)$$

The generalized solutions of an example are presented in Table 1.

Table 1. Generalized solutions of an example

$\overline{u}_{h\,max}$ [m²/kN]	$\overline{Q}_{max}$ [/]	$\overline{M}_{max}$ [/]
$17.17 \cdot 10^{-6}$	$-152.53 \cdot 10^{-3}$	$63.52 \cdot 10^{-3}$

On the basis of equations (8), (9) and (10) we determined the values of the maximum displacement and of the inner forces which are shown in Table 2.

Table 2. Results of the practical problem obtained from the generalized solutions

$u_{h\text{-}max}$ [mm]	Q_{max} [kN/m]	M_{max} [kNm/m]
8.60	-76.20	158.80

The verification of the results was performed by geotechnical analyses considering real geometrical and geotechnical data presented in Figure 10. The results of this analysis are shown in Table 3.

Table 3. Results of the analysis of a practical problem

$u_{h\text{-}max}$ [mm]	Q_{max} [kN/m]	M_{max} [kNm/m]
9.30	-72.31	154.67

The comparison of the results from Table 2 and Table 3 shows us that the difference is less than *8 %*, which is within permissible limits.

8. DESIGN DIAGRAMS

The design values of the soil, structure and loading characteristics are determined from their characteristic values using partial and model factors which are defined by standards. The design friction angle is reduced to a failure friction angle which is equal to the asymptote value of the lines in the diagrams. It is defined as:

$$\varphi_p = arc \, tan \big(tan \, \varphi_k / \gamma_\varphi \big) \qquad (11)$$

where γ_φ denotes the safety factor for the friction angle, its value depends on the standard. If we use the Eurocode standard which prescribes the safety factor of $\gamma_\varphi = 1.25$, it is possible for all models to represent the design values of the displacement and the inner forces of the retaining structure. Figure 11 represents the design values of generalized displacements for Model I.
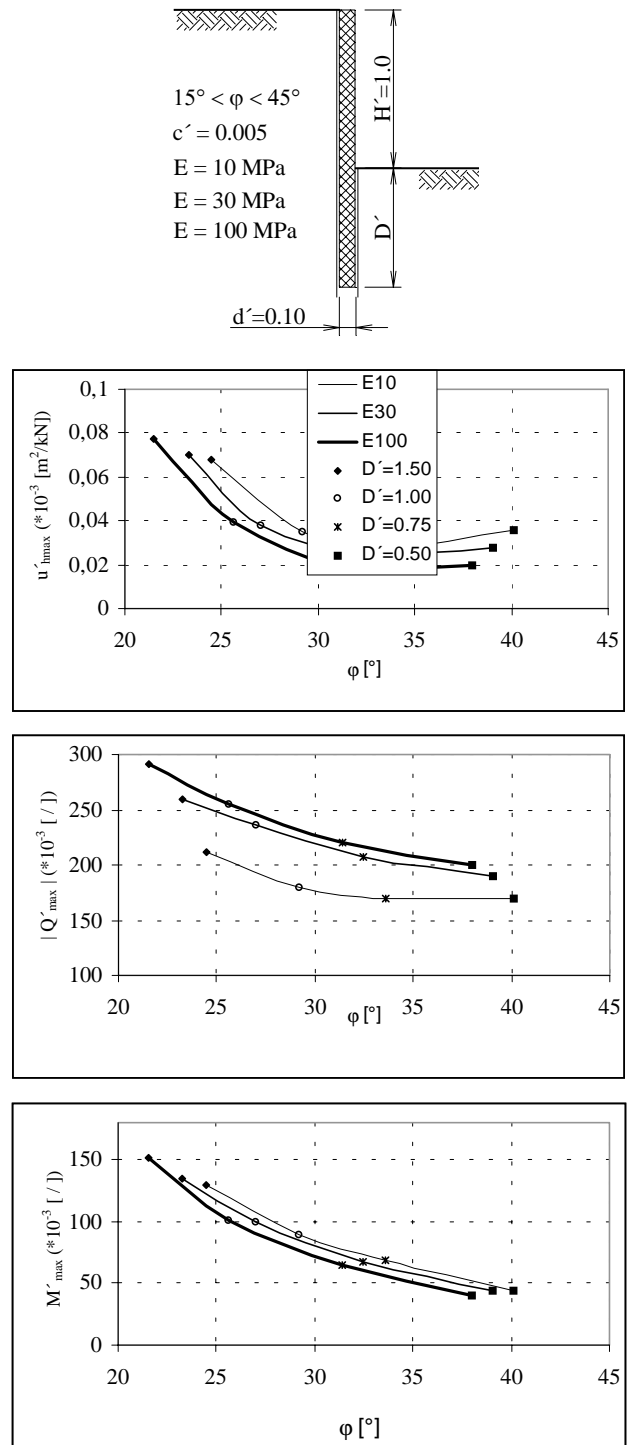
Fig. 11 Design values of generalized displacements and inner forces for a safety factor $\gamma_\varphi = 1.25$

9. CONCLUSION

This paper presents a new approach to the determination of the interdependence between load and movements of the embedded retaining structure in the geotechnical practice. This approach is based on the results of an analysis of interaction using a generalized soil-structure model which may easily be used in practice for simple constitutive relationships between loads and soil deformations.

The results of the research, as given in Figures 6, 7 and 9, show that the anticipated deformations of the soil-structure system are not significantly influenced by the friction angle, when $35° < \varphi < 45°$. We have to point out that cohesion of the soil has a favorable influence on the structure deformation and inner forces, especially for lower values of the friction angle.

This paper presents a non-linear interaction only for certain combinations of the soil characteristics. All presented results have been evaluated using an isotropic Hardening-Soil model.

According to the presented research we can conclude that the use of contemporary software and suitable input parameters enables us to determine generalized non-linear solutions of the soil-structure interaction in the form of diagrams. These diagrams can be used for the solution of simple geotechnical problems.

10. REFERENCES

[1] W.C. Rheinholdt and E. Riks, Solution techniques for non-linear finite element equations, In: State-of-the-art Surveys on Finite Elemet Techniques, Eds. A.K. Noor and W.D. Pilkey, Chapter 7, 1986.

[2] T. Schanz, P.A. Vermeer and P.G. Bonnier, Formulation and verification of the hardening-soil model, Submitted for publication to *Int. Journal of Numerical and Analitical Methods in Geomechanics*, 1999.

[3] W. Powrie and E.S.F. Li, Finite element analyses of an in situ structure propped at formulation level, *Geotechnique*, Vol. 41, No. 4, pp. 499-514, 1991.

[4] S. Škrabl, Interaction between hinge-tied foundation structures and soil, Ph.D. Thesis, University of Maribor, Faculty of Civil Engeenering, Maribor, 1991.

[5] S. Škrabl, Bearing capacity and settlement of vertically-loaded piles, Proc. of the International Congress on Deep Foundations, ASCE, Orlando, Florida, 2002.

[6] R.B.J. Brinkgreve and P.A. Vermeer, Plaxis - Finite element code for soil and rock analyses, Ver. 7, A.A. Balkema, Rotterdam-Brookfield, 1998.

[7] T. Schanz and P.A. Vermeer, On the stiffness of sands, *Geotechinque*, Vol. 48, pp. 383-387, 1998.

[8] R.L. Kondner, A hyperbolic stress strain formulation for sands, Proc. 2nd Pan. Am. ICOSFE, Brazil, Vol. 1, pp. 289-324, 1963.

[9] M. Duncanv and C.Y. Chang, Nonlinear analysis of stress and strain in soil, *ASCE Journal of the Soil Mechanics and Foundation Division*, Vol. 96, pp. 1629-1653, 1970.

[10] L. Trauner and H. Vrecl, The outline for analysis of soil-structure interaction, *Bulletins for Applied Computing Mathematics*, PAMM, Budapest, 2000.

[11] S. Škrabl and L. Trauner, The constitutive parameters of soft claystone, *Bulletins for Applied Computing Mathematics*, PAMM, Budapest, 1999.

PARAMETARSKA NELINEARNA ANALIZA UKOPANE POTPORNE STIJENE

SAŽETAK

U članku je predstavljen opći model interakcije između potporne stijene i tla. Prikazano rješenje se bazira na elasto-plastičnoj analizi interakcije između potporne stijene i nelinearnog tla. Ravninski model građevine i tla analiziran je metodom konačnih elemenata. Na osnovu rezultata analitičkih rješenja i numeričkih analiza napravljen je opći model interakcije između potporne stijene i tla. Najveće značenje predloženog modela temelji se na svojstvu da su deformacije i unutrašnje statičke veličine stijene s različitim karakteristikama tla kao i geometrijski podaci dobiveni generalizirano na temelju konačnog broja rezultata nelinearnih analiza [1]. Rezultati istraživanja dani su u dijagramima.

Drugi dio rada prikazuje primjer stvarnog geotehničkog problema s provjerom generaliziranih rezultata te prijedlog uporabe općeg rješenja kod projektiranja.

Ključne riječi: *interakcija tla i konstrukcije, potporna građevina, elasto-plastična analiza, nelinearna analiza.*